Available online at www.sciencedirect.com

ScienceDirect

Advances in Space Research 71 (2023) 5185–5195

ADVANCES IN SPACE RESEARCH
(a COSPAR publication)

www.elsevier.com/locate/asr

Latitudinal responses of the ionosphere over South America during HILDCAA intervals: Case studies

Regia Pereira Silva [a,*], Clezio Marcos Denardini [a], Láysa Cristina Araújo Resende [a], Juliano Moro [b], Jonas Sousasantos [c], Carolina de Sousa do Carmo [a], Sony Su Chen [a], Paulo França Barbosa Neto [d], Giorgio Arlan da Silva Picanço [a], Jaziel Felipe Braga Campelo [e], Gilvan Luiz Borba [e], Marcos Aurélio Ferreira dos Santos [f]

[a] *National Institute for Space Research – INPE, 12227-010, São José dos Campos, SP, Brazil*
[b] *State Key Laboratory of Space Weather, Beijing, China*
[c] *William B. Hanson Center for Space Sciences, University of Texas at Dallas (UTD), Richardson, TX, USA*
[d] *Salesian University Center of São Paulo – UNISAL, Lorena, SP, Brazil*
[e] *Federal University of Rio Grande do Norte – UFRN, Natal, RN, Brazil*
[f] *Northeast Space Coordination – COENE/INPE, Natal, RN, Brazil*

Received 8 August 2022; received in revised form 23 December 2022; accepted 11 February 2023
Available online 15 February 2023

Abstract

Aspects regarding the influence of High-Intensity Long-Duration Continuous Auroral Electrojet Activity (HILDCAA) intervals on ionospheric dynamics have been objecting to increasing interest in the last years. Notwithstanding, some key interconnections between the HILDCAA intervals impacts on the ionosphere over distinct latitudes, according to the solar cycle phase, remain to require further investigation. In this work, the F2 layer peak height and its critical frequency (hmF2 and foF2, respectively) from Digisonde data obtained over São Luís (2.60° S; 44.21° W), Cachoeira Paulista (22.70° S; 44.98° W), and Port Stanley (51.60° S, 57.9° W), were evaluated to unravel more details of the ionospheric responses to four HILDCAA intervals as case studies. Those are equatorial, low, and mid-latitude stations, respectively, and the main results over them presented a similar trend in terms of solar cycle dependence, with the greater impact on the ionospheric density along with solar maximum conditions, despite the higher frequency of HILDCAA occurrences in the descending and minimum phases. The variation of hmF2 due to HILDCAA effects in comparison to quiet time is about 20% in equatorial and mid-latitudes, while over the low latitude station the hmF2 ranges positively up to 40%. These results enhance our understanding of the HILDCAAs magnitude degree both regarding its solar cycle occurrence, and its effects in different ionospheric latitudinal sections.

Keywords: HILDCAA; Ionosphere; Electron density peak; Electron density altitude; Solar cycle

* Corresponding author at: INPE/DICEP, Av. dos Astronautas, 1758, Jd. da Granja, 12227-010, São José dos Campos, SP, Brazil.
E-mail addresses: regiapereira@gmail.com, regia.pereira@inpe.br (R.P. Silva), clezio.denardin@inpe.br (C.M. Denardini), laysa.resende@inpe.br (L. C.A. Resende), juliano.moro@inpe.br (J. Moro), jonas.ssts@utdallas.edu (J. Sousasantos), carolina.carmo@inpe.br (Carolina de Sousa do Carmo), sony.chen@inpe.br (S. Su Chen), pafraneto@gmail.com (P. França Barbosa Neto), giorgio.picanco@inpe.br (Giorgio Arlan da Silva Picanço), jaziel.f.b.campelo@gmail.com (J.F.B. Campelo), gilvan.borba@ufrn.br (G.L. Borba), marcos.aurelio@inpe.br (Marcos Aurélio Ferreira dos Santos).

https://doi.org/10.1016/j.asr.2023.02.020
0273-1177/

1. Introduction

In recent years, there is a noteworthy interest in space weather events and phenomena that occur more frequently in the solar cycle minimum phase, which generally have moderate or weak effects on the Earth's environment. High-Intensity Long-Duration Continuous Auroral Electrojet Activity (HILDCAA) behaves as this type of event. Tsurutani and Gonzalez (1987) first used the term in their study when they examine 500 days of AE and Dst indices in order to select intervals of high-intensity auroral activity that occur outside of the magnetic storms main phase. Later, some studies showed that HILDCAA occurrences do not depend on a geomagnetic storm preceding it (Tsurutani et al., 2004; Gonzalez et al., 2006), and are more likely to occur in the descending and minimum phases of the solar cycles (Hajra et al., 2013; 2014).

HILDCAA intervals are usually defined according to the following guidelines: (i) the Auroral Electrojet (AE) index peak must exceed 1000 nT at least one time during the event; (ii) the AE values never drop below 200 nT for more than 2 h during the event; (iii) the duration of the perturbation is greater than two days, and (iv) its occurrence must be separate from magnetic storms main phases (Tsurutani and Gonzalez, 1987) In the pioneer study, the chosen classification criteria for HILDCAAs were empirical since one wanted to illustrate the distinct aspects noticed during the phenomenon. However, the same physical process may occur when one or more criteria are not strictly observed (Tsurutani et al., 2004). Therefore, in the current study, high AE index activity was considered during the HILDCAA interval, even in cases when it eventually dropped to values below 200 nT for more than 2 h.

HILDCAAs are caused by the southward components of the Alfvén wave train present in the High-Speed Streams (HSS) mainly. During these events, energy and accelerated energetic particles are continuously injected into the magnetosphere through magnetic field reconnection (Tsurutani et al., 1994, 1995, Balogh et al, 1995, Søraas et al,.2004; Sandanger et al., 2005, Hajra et al, 2014). The continuous magnetic reconnection may last for days to weeks, causing perturbations in the magnetosphere-ionosphere coupling.

Regarding HILDCAAs impact on the ionosphere, some studies have been done in the last decades. Sobral et al. (2006) showed a significant coupling process between the auroral zone and the equatorial ionosphere during HILDCAAs. (Koga et al., 2011) analyzed a five days HILDCAA event. The authors observed a positive (negative) correlation of the plasma drift vertical component with the interplanetary and reconnection electric fields during daytime (nighttime) for an equatorial station. Silva et al. (2017) and Yeeram and Paratrasri (2018) reached the conclusion the changing of the auroral electron density due to HILDCAAs impact may be mapped to equatorial and low-latitude ionosphere through electric fields disturbances as prompt penetration electric fields and disturbance dynamos. De Siqueira et al. (2017) in a study comprising HILDCAAs and geomagnetic storms over South America analyzed the ionospheric Total Electron Content (TEC) responses for geomagnetic storms followed by HILDCAAs. They notice intense TEC increases for the HILDCAAs compared to the geomagnetic storms preceding these events. Silva et al. (2020) investigated the HILDCAA disturbance time effects in the TEC values for equatorial and low latitudes, using a sample of 10 HILDCAA intervals. The authors identified a predominance of positive ionospheric storms (i.e., electron density increase) and seasonal features as equinoctial anomalies in HILDCAA intervals that have occurred in different seasons.

These previous works about the HILDCAAs impact on the ionosphere were very suitable for clarifying some lacks regarding HILDCAAs-ionosphere coupling. However, some other aspects remain unclear. For instance, the previous works do not explain how the effects of HILDCAAs are manifested according to which solar cycle phase those intervals occur and how distinct latitudes experience such effects.

In this work, four HILDCAA intervals were chosen as case studies to cover the distinct phases of the solar cycle, namely, solar maximum, descending phase, solar minimum, and ascending phase. The case studies also consider three different latitudinal sectors in South America using equatorial, low, and mid-latitude stations, hence, evaluating the latitudinal responses to the HILDCAAs in different stages of the solar cycle.

2. Data and methodology

This paper outlines the latitudinal ionospheric responses to HILDCAA intervals that occurred during distinct phases of the solar cycle phase. The work considers three different latitudinal sectors in South America.

Four HILDCAA intervals under distinct solar cycle phases were chosen for this study. Table 1 shows details of the events under evaluation. The numbers in the left column refer to HILDCAA intervals identification (ID), the central column indicates the date range, and the right column their respective solar cycle phase of occurrence. The intervals were chosen following the criteria used to identify the HILDCAAs, as mentioned in the previous section. The geomagnetic indexes and the z component of the interplanetary magnetic field (IMF Bz) were obtained from OMNIWeb Plus data and service (https://omniweb.gsfc.nasa.gov/ow.html).

Table 1
List of HILDCAA intervals.

ID	Date range (yyyy/mm/dd – dd)	Solar cycle phase
H01	2000/02/05 – 09	Solar maximum
H02	2006/03/18 – 22	Descending phase
H03	2008/06/15 – 18	Solar minimum
H04	2010/04/05 – 08	Ascending phase

The ionospheric parameters used in this study were the F2 layer critical frequency (foF2) and the electron density peak height (hmF2) obtained by three ground-based digital ionosonde. Their geographic locations are São Luís (SL, 2.60° S; 44.21° W), Cachoeira Paulista (CP, 22.70° S; 44.98° W) and Port Stanley (PS, 51.60° S, 57.9° W) as shown in Fig. 1. One additional digital ionosonde deployed at Fortaleza (FZ, 3.90° S, 38.40° W) was used during the solar minimum event due to a lack of data from SL ionosonde. The critical frequency is associated with the electron density, while the altitude of the peak density in the F2 layer is an indication of ionospheric electric field variations.

The digital ionosondes used are Digisondes DPS (Digital Portable Sounders) that measure the time of flight of the pulse-modulated HF signals, ranging from 1 to 30 MHz with a 25 kHz frequency step. The soundings repeat and ionospheric echoes received are continuous in a temporal range, generally 15 min, but can be different for each station since the sequence of soundings is selectable (Reinisch, 1986; Reinisch et al., 2005, 2009). All ionograms used in this study were manually scaled using the SAO-Explorer, a Digisonde data analysis tool available in https://ulcar.uml.edu/SAO-X/SAO-X.html.

The ionospheric parameters during the HILDCAA disturbed days were compared with average values calculated based on three days belonging to a quiet period around each event, in order to mitigate the day-to-day variability. The quiet days for reference were chosen within fifteen days around each HILDCAA interval, from planetary K index (Kp), which data were obtained from the World Data Center for Geomagnetism, Kyoto, Japan (https://wdc.kugi.kyoto-u.ac.jp/index.html). In this work, the daily sum of Kp ($\sum$Kp) was used to evaluate the geomagnetic conditions, since the three quietest days were chosen from the lowest $\sum$Kp values. Beyond that, to interpret the HILDCAA effects on the ionosphere along the latitudes, we analyzed data from stations within a longitudinal window of 20°, hence; avoiding large differences regarding the ionization processes (see the shaded area in Fig. 1).

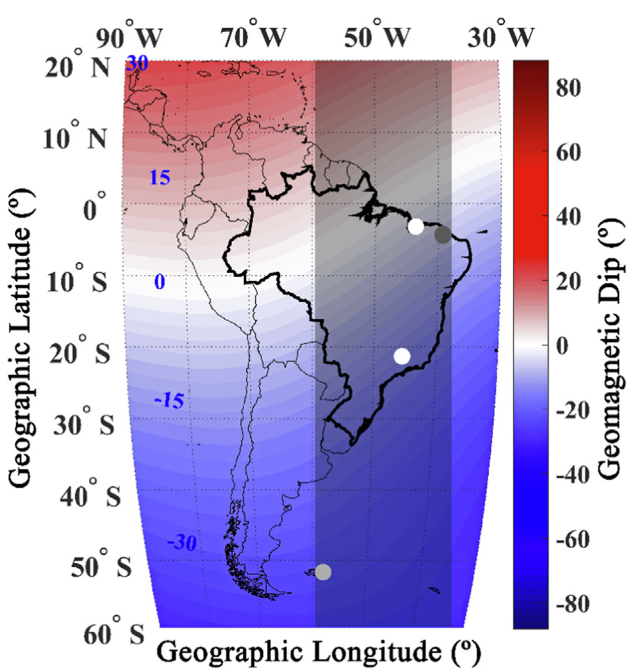

Fig. 1. The white dots in the map show the Digisonde stations used in this study, which are São Luis (equatorial station), Cachoeira Paulista (low latitude station) and Port Stanley (middle latitude station). The grey dot refers to Fortaleza (equatorial station) used in this study for solar minimum phase. The shaded area represents the longitude limit defined in this study.

The ionospheric parameters foF2 and hmF2 during the HILDCAA intervals, $foF2_H$ and $hmF2_H$, respectively, were compared with quiet values for reference using percentage variance (V%) according to Equations (1) and (2):

$$foF2_{V\%} = [(foF2_H - foF2q)/foF2q] \times 100 \quad (1)$$

$$hmF2_{V\%} = [(hmF2_H - hmF2q)/hmF2q] \times 100 \quad (2)$$

where foF2q and hmF2q indicate the reference values for quiet time. The aim is to analyze the percentage changes between the HILDCAAs disturbed days and the quiet period of reference.

In the next section, we will address ionospheric variability both in the way it presents during HILDCAAs and in terms of percentages. Then, a comparison of the latitudinal responses during different solar cycle phases will have presented.

3. Results and discussion

The variability of $foF2_H$ and $hmF2_H$ parameters during the HILDCAA intervals are shown in Figs. 2 and 3. These Figures depict the $foF2_H$ (red dots) and $hmF2_H$ (blue dots) in relation to quiet values (grey dots). All days belonging to the HILDCAA disturbance time were plotted jointly. Each panel in Figs. 2 and 3 refers to an individual phase of the solar cycle. The top panels refer to the solar maximum (left) and descending phase (right), whereas the bottom panels refer to solar minimum (left) and ascending phase (right). The vertical axis is MHz in Fig. 2, and km in Fig. 3, while the horizontal axis is in Universal Time.

The ionospheric variabilities seen in Figs. 2 and 3 reveal a known feature, mainly in the equatorial and low-latitude ionosphere, i.e., the disturbances caused by HILDCAA events generally range from weak to moderate magnitudes when compared to intense geomagnetic storms (Sobral et al., 2006, Silva et al., 2017, 2020, De Siqueira et al., 2017). To understand the magnitude degree of HILDCAAs since the way these intervals impact the ionospheric responses according to each phase of the solar cycle, the percentage variance from ionospheric parameters, $foF2_{V\%}$ and $hmF2_{V\%}$, was taken.

Figs. 4 and 5 present the results of $foF2_{V\%}$ and $hmF2_{V\%}$, respectively. Each Figure was organized in four panels according to the solar cycle phase. Each panel presents three plots for all latitudinal stations used in this study,

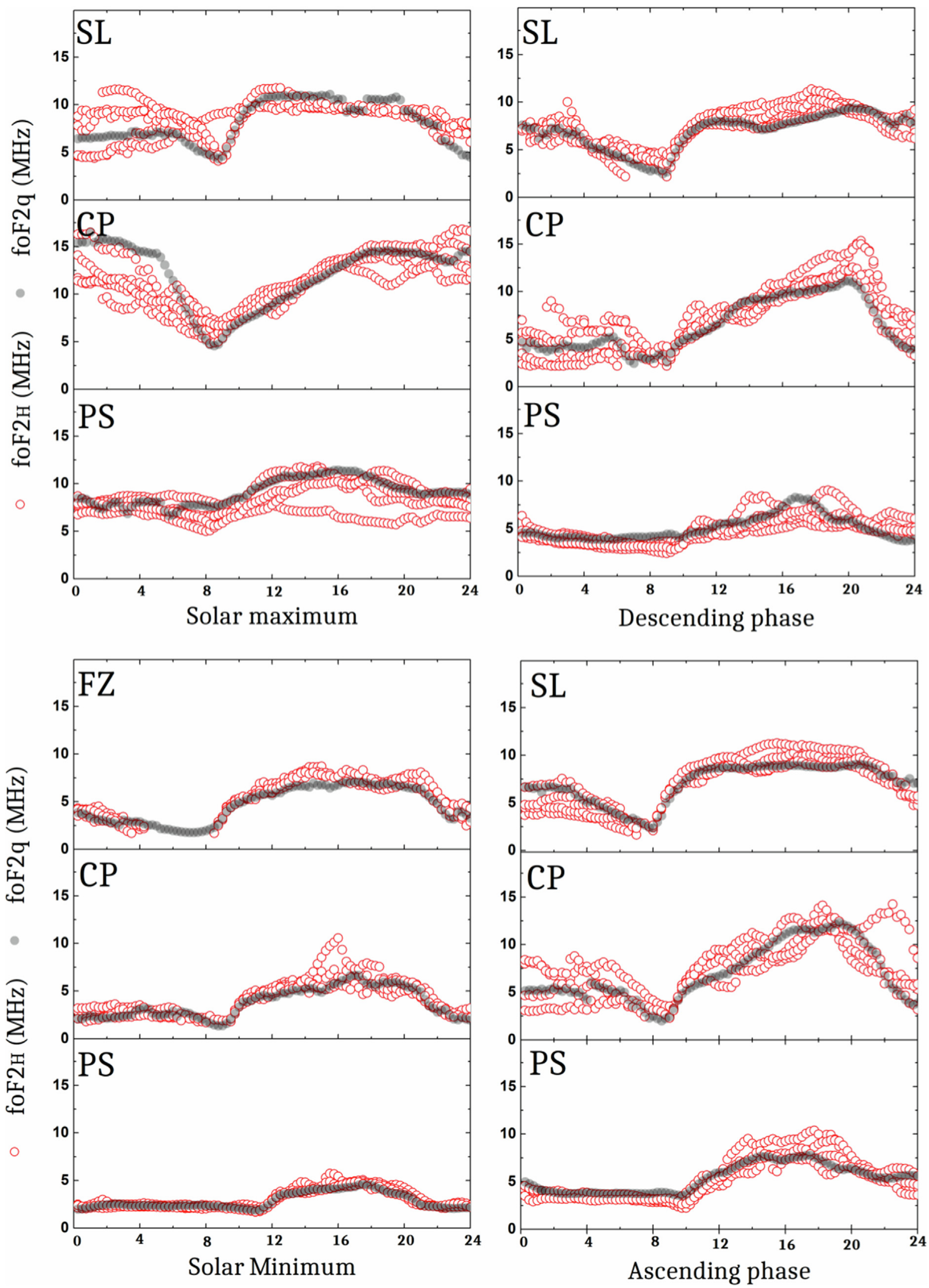

Fig. 2. F2 layer critical frequency during disturbed ($foF2_H$) and quiet days (foF2q) in the Digisonde stations used in this study.

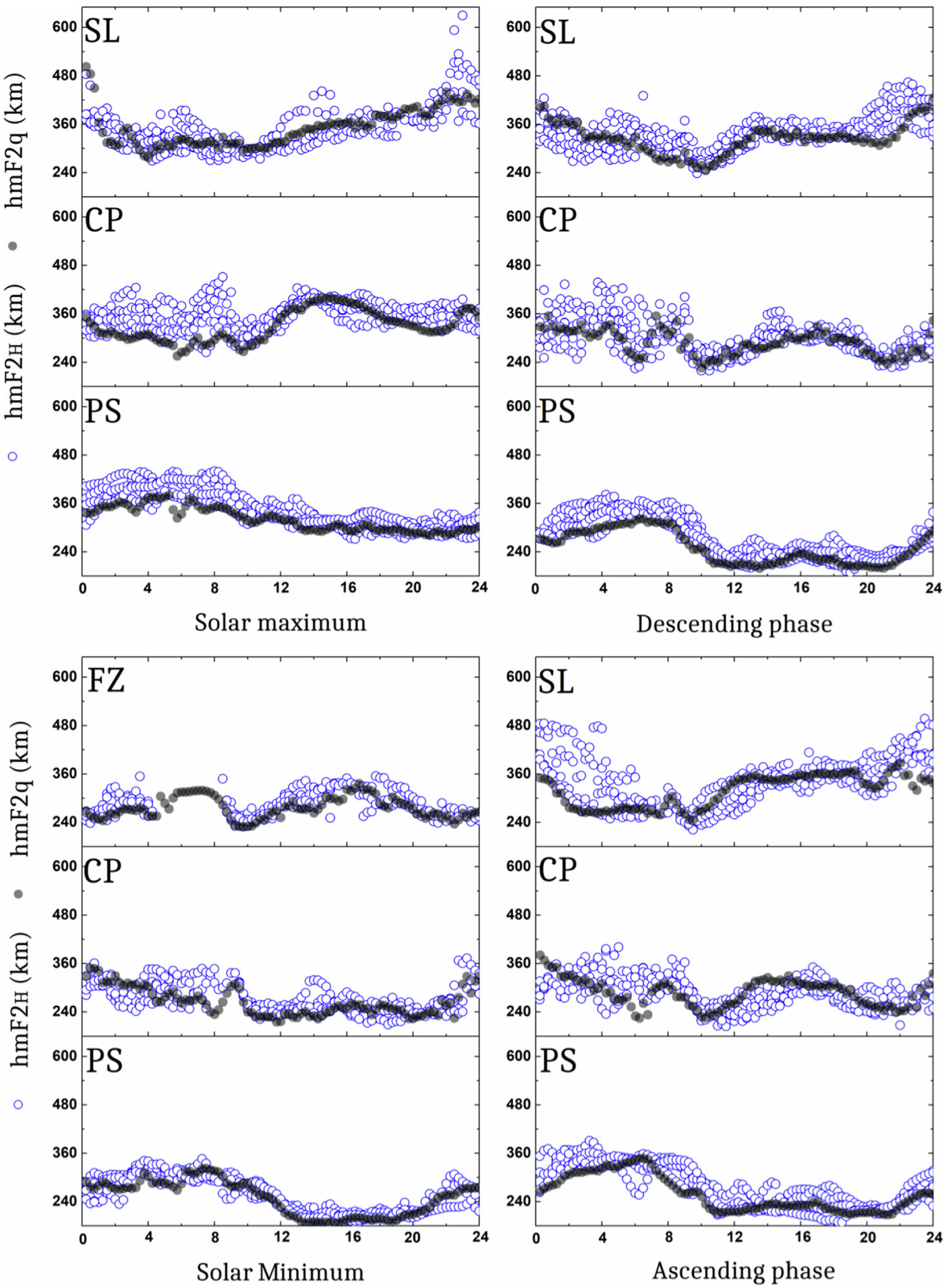

Fig. 3. F2 layer height of the peak electron density during disturbed ($hmF2_H$) and quiet days (hmF2q) in the Digisonde stations used in this study.

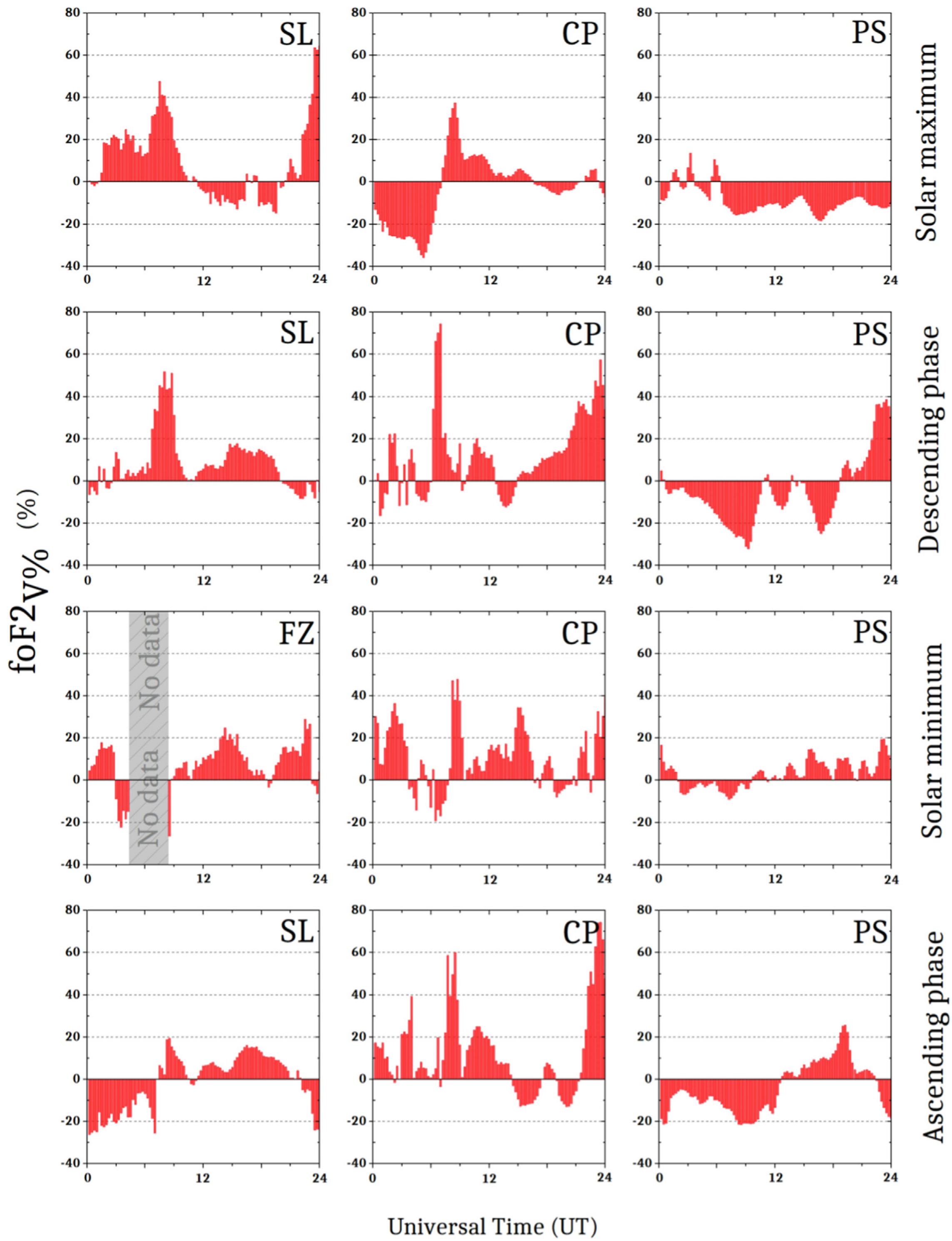

Fig. 4. Percentage variance of foF2 parameter ($foF2_{V\%}$) during the HILDCAA intervals.

namely, SL; CP; and PS. Data from FZ were used as the equatorial station in the panel dealing with solar minimum interval, as mentioned previously. Similar to Figs. 2 and 3, all days belonging to the HILDCAA disturbance time were plotted jointly. The vertical axis refers to percentage values, while the horizontal axis is the Universal Time. Analyzing each case for all the four solar cycle phases, the responses of the ionospheric parameters to the HILDCAAs activity are clearly noticed. Generally, the responses of the foF2 parameter are predominantly positive, with considerably less occurrence of negative responses. In Fig. 4, it is possible to see positive responses reaching more than 70% during some hours compared to quiet values, while the negative changes occasionally surpass 30%. The positive

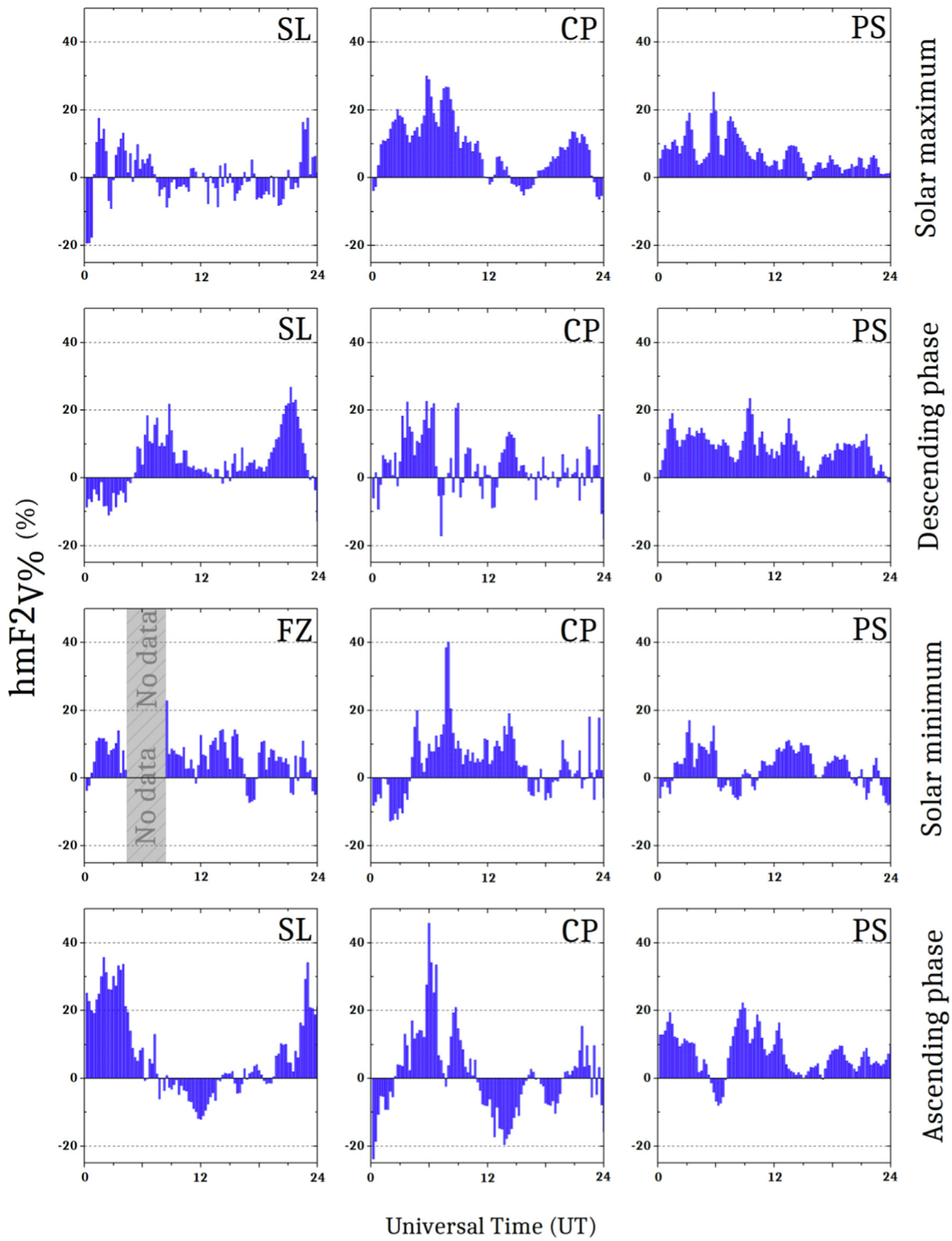

Fig. 5. Percentage variance of hmF2 parameter ($hmF2_{V\%}$) during the HILDCAA intervals.

values are more evident over equatorial and low-latitude regions; meanwhile, the mid-latitude station recorded mainly negative responses. These results indicate that HILDCAAs impacts are mostly positive in the equatorial and low-latitude ionospheric foF2. This fact is corroborated by the analysis from the ionospheric total electron content (TEC) during ten HILDCAA intervals presented by Silva et al. (2020), in which the authors found a prevalence of the positive ionospheric storms. However, when analyzing each latitudinal station, it is possible to notice that those positive effects do not happen in all locations. The exception was Port Stanley. The mid-latitude station presents negative responses almost the entire solar cycle, except for the solar minimum phase, since the $foF2_{V\%}$ is very low, but predominantly positive, in comparison with the responses for the same station during other phases of the solar cycle.

Fig. 5 depicts the $hmF2_{V\%}$ values and suggests a great variability in this parameter. The percentage variance reveals that the HILDCAAs effects on hmF2 oscillate around 20%, between positive and negative values, recurrently. Few exceptions occur in CP during the solar minimum and ascending phases, which it is possible to see the $hmF2_{V\%}$ reaching and overtaking 40%. The difference in the elevation of the F2 ionospheric layer between CP and SL during HILDCAAs was already observed by Sobral et al. (2006). In their analysis, they suggest the uplift of the F layer over CP is caused by high-intensity AE generating disturbance equatorward winds similar to those observed during geomagnetic storms.

It is important to note the hmF2 was rarely suppressed at PS or had a negative response, even with a behavior very similar to the quiet day reference profile seen at the bottom panels of Fig. 3. These results are noteworthy, and we believe that this is a new aspect not revealed up to now.

The variability seen in the ionospheric parameters is related with the energy transfer during HILDCAAs activity. The magnetic reconnection is the main mechanism of energy transfer between the solar wind and Earth's magnetosphere during geomagnetic activities, but it is not the only one. During HILDCAAs activity, a persistent injection of ions and energetic electrons in the ring current is one of the causes of the extended energization, beyond inhibiting the normal decay of the ring current, delaying the time to reach the values of the quiet conditions (Søraas et al., 2004; Sandanger et al., 2005; Gonzalez et al., 2006). Another important factor is the particle precipitation in the auroral oval during the day sector. Guarnieri (2006) used images from POLAR satellite to show that during HILDCAA intervals there is a continuous photon emission throughout the auroral oval, differently from what occurs in geomagnetic storms and substorms. The constant penetration of energy during HILDCAAs modifies the configuration of electric fields, consequently, changing the height and the density peak of the F2 layer. As HILDCAA is a long-lasting event is expected persistent changes in the ionosphere. Once the injection of energy is continuous during this kind of geomagnetic activity the global thermospheric circulation and the ionization density at F region heights are altered. Initially, the perturbations are seen in high-latitude as pointed out by Guarnieri (2006) when he observed low-intensity auroras over the entire auroral oval; from dayside to nightside as a strong indication that solar wind-magnetosphere interaction is a complex and global one during these events. Both prompt penetration and disturbance dynamo electric fields may occur during HILDCAA intervals. These electric fields are mapped along geomagnetic field lines from high to middle and low latitudes. At time these electric fields penetrate to lower latitudes, they are responsible for the ionospheric storms seen by the foF2 parameter.

Regarding PS ionospheric responses, Figs. 4 and 5 show that the $foF2_{V\%}$ is predominantly negative while the $hmF2_{V\%}$ is positive, indicating that the F region has lifted during HILDCAAs, however, the density apparently decayed. Beyond disturbance dynamo effects in PS negative ionospheric storms, the ionosphere over the mid-latitude is intrinsically coupled with the plasmasphere. When some space weather activities happen, as geomagnetic storms or HILDCAAs, the F layer can raise up to higher altitudes, and the [O]/[N] ratio may decrease since the oxygen interacts with hydrogen gas via charge exchange reaction decreasing the plasma density.

In order to compare the ionospheric responses to HILDCAAs activity over specific latitude sectors through solar cycle phases, Figs. 6 and 7 were prepared. Both figures present the average values of the parameters $foF2_H$ and $hmF2_H$ ($\overline{foF2}_H$ and $\overline{hmF2}_H$), separately, for each HILDCAA interval occurred in each solar cycle phase. The top, central and bottom panels refer to equatorial, low, and mid-latitude stations, respectively. The red, green, blue, and black colors indicate the maximum, descending, minimum, and ascending phases of the solar cycle, respectively. One interesting aspect of this analysis is observing in Fig. 6 the average values of the ionospheric density during

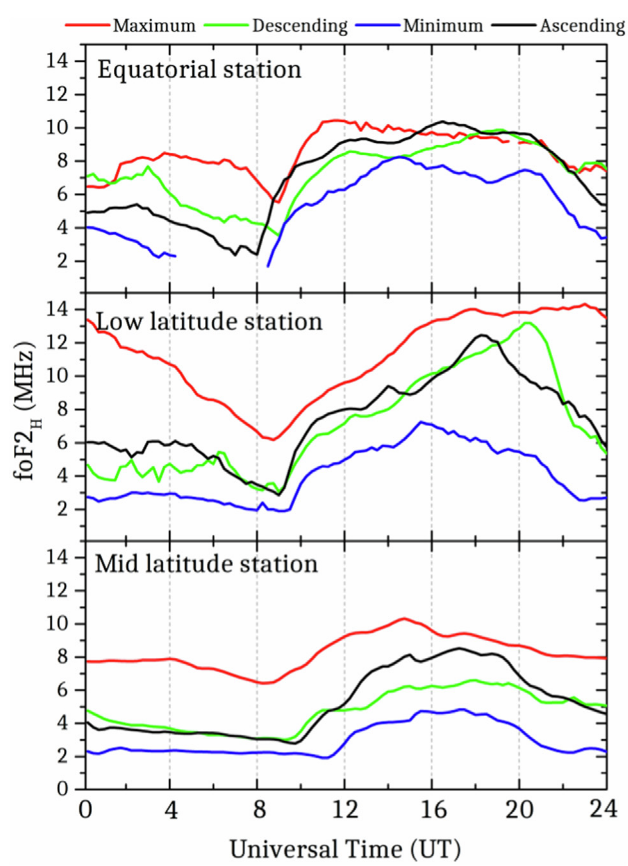

Fig. 6. Mean values of the parameter $foF2_H$ for equatorial (upper panel), low (center panel), and middle (bottom panel) latitudes. The colors red, green, blue, and black indicate the maximum, descending, minimum, and ascending solar cycle phases, respectively.

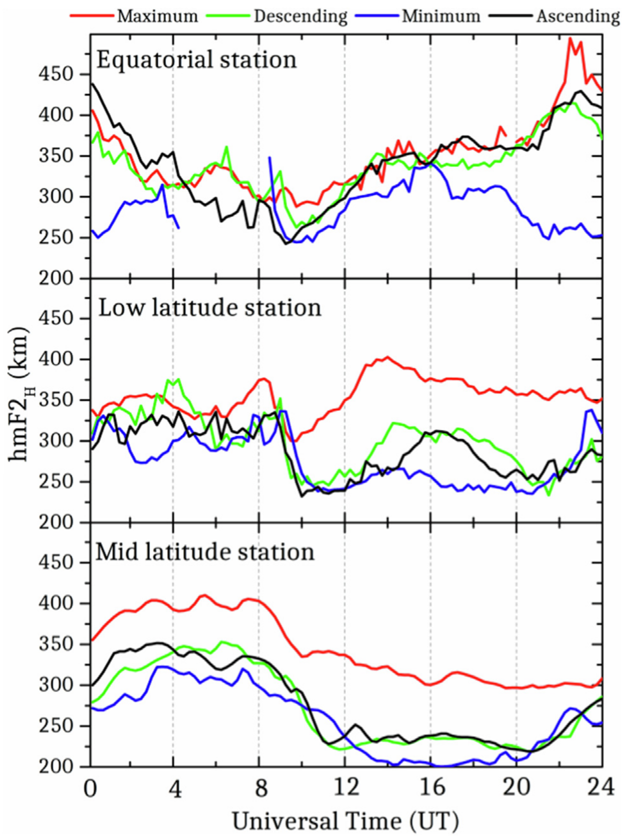

Fig. 7. Same as Fig. 6 but for the $hmF2_H$.

HILDCAA events compared with the respective quiet reference values, according to Equation (1). For the cases of HILDCAA intervals studied here, it is possible to perceive a relationship of solar cycle dependence, since the highest values occur at solar maximum, even with the lowest rate of occurrence of this kind of event being in the solar maximum (Hajra et al., 2013). Another analysis regards latitudinal dependence. The low-latitude ionosphere presents larger values of electron density during HILDCAA activity similar to what happens in this same region during geomagnetic storms (Mendillo, 2006; Abdu et al., 2008; Liu and Chen, 2009; De Siqueira et al., 2011; Jonah et al., 2015). The mid-latitude station presented modest values compared to the other stations analyzed here. However, it is interesting to note that $fo\bar{F}2_H$ values during the solar maximum are similar over the equatorial and mid-latitude stations. These situations analyzed here show us that the latitudinal location is an important factor for the ionospheric density during HILDCAA disturbance time.

Due to the prolonged duration characteristic of HILDCAA events, its impacts may be mitigated or diluted along time. In this context, the variation of the ionospheric density due to latitudinal conditions may play an important role during the occurrence of the event, unless there is a punctual and strong input of energy or penetration of electric fields.

Fig. 7 shows a great variation in the mean values of $hmF2_H$. The equatorial station presents an uplift of the F2 layer during HILDCAA disturbance time for all solar cycle phases, while over the low-latitude station the F layer elevation is more distinguished in the solar maximum. Silva et al. (2017) and Yeeram (2019) studied the ionospheric electric fields configuration during HILDCAAs. Their studies pointed out the important role of the prompt penetration and disturbance dynamo electric fields occurrences during HILDCAAs. Wei et al. (2008) reported that multiple electric field penetration to equatorial ionosphere is associated with HILDCAAs, and Silva et al. (2017) have suggested that the equatorial hmF2 response is related to interplanetary electric field penetration. This could explain the high values of the electron density peak height in this latitudinal region during the HILDCAA interval.

The F layer height response over mid-latitudes seems to be dependent on the solar cycle since the highest values occurred during solar maximum and the lowest values occurred, predominantly, during solar minimum. The main process that explains the height changes in the mid-latitude ionosphere during geomagnetic activities is the heating of the high-latitude thermosphere, generating horizontal disturbed winds that migrate equatorward. These winds, in turn, may move the ionospheric plasma along the magnetic field lines and raise the ionospheric peak height (Prölss and Očko, 2000; Fedrizzi et al., 2008; Blanch and Altadill, 2012). On the one hand, during HILDCAA activity the input of energy is not strong and punctual in the high latitudes heating the auroral region by Joule dissipation as geomagnetic storms. Generally, the input of energy is extensive but attenuated and long-lived. During HILDCAAs the energization of the ionosphere-magnetosphere coupling occurs continuously, and, sometimes, it can be more effective according to the polarity that Bz presents.

These findings presented in this work provide insights for future statistical analysis further investigating the intensity and the effects of HILDCAA events on the ionosphere.

4. Concluding remarks

It has been presented in this paper four case studies about latitudinal ionospheric responses to HILDCAA intervals, which occurred across the different phases of the solar cycle, using three Digisonde deployed at equatorial, low, and mid-latitude regions. The main results are summarized as follows.

Some answers were found in terms of hmF2 and foF2 ionospheric parameters in equatorial, low and middle latitudes. HILDCAA effects on hmF2 range around 20%, between positive and negative values in the equatorial latitude while in the low-latitude the hmF2 ranges positively up to 40% in some hours of the day. In toward foF2 responses to HILDCAAs, the parameter presented predominantly positive changes, since it reaches 70% in comparison to the quiet pattern while the negative responses occasionally surpass 30%. This feature was especially verified over equatorial and low latitudes. Regarding the mid-latitude station, the foF2 presented negative responses almost the entire solar cycle.

Another important analysis done in this study refers to the ionosphere reactions according to HILDCAA occurrences in different solar cycle phases. All latitude sites studied here presented a similar trend in terms of solar cycle dependence, with less impact on the ionospheric density during the solar minimum, while the stronger impact occurred during the solar maximum. The latter is a very interesting comportment since the highest rates of occurrence of HILDCAAs are during the descending and minimum phases. For the cases studied here, this feature suggests that the impacts of HILDCAAs on the ionosphere are solar cycle dependent.

5. Availability of data and materials

The geomagnetic indexes and the southward component of the interplanetary magnetic field (IMF Bz) are available in OMNIWeb Plus data and service (https://omniweb.gsfc.nasa.gov/ow.html). The planetary K index (Kp) data were obtained from the World Data Center for Geomagnetism, Kyoto, Japan (https://wdc.kugi.kyoto-u.ac.jp/index.html). Data from the Brazilian Ionosonde network (São Luís and Cachoeira Paulista) is made available through the EMBRACE program from the National Institute for Space Research (INPE) (https://www2.inpe.br/climaespacial/portal/ionosondes-home/). Data from digisonde installed in Port Stanley is available by Global Ionosphere Radio Observatory (GIRO) at DIDBase GIRO web Portal (https://ulcar.uml.edu/DIDBase/).

Funding

We are thankful for the support from Conselho Nacional de Desenvolvimento Científico e Tecnológico (CNPq/MCTI) through the Grants 302000/2021–6, 300324/2022–7, 302675/2021–3, 429517/2018–01, 141935/2020–3 and 123663/2021–0; Coordenação de Aperfeiçoamento de Pessoal de Nível Superior (CAPES/MEC) through the Grants 88887.362982/2019–00 and 88887.351778/2019–00; Fundação de Amparo à Pesquisa do Estado de São Paulo (FAPESP) through the Grant 2018/06158–9; and NSF award AGS-1916055.

Declaration of Competing Interest

The authors declare that they have no known competing financial interests or personal relationships that could have appeared to influence the work reported in this paper.

Acknowledgements

Regia P. Silva acknowledges the supports from Conselho Nacional de Desenvolvimento Científico e Tecnológico (CNPq/MCTI) through the Grants and 302000/2021-6 and 300324/2022-7. C. M. Denardini thanks to CNPq/MCTIC (Grant 302675/2021-3). L. C. A. Resende and J. Moro would like to thank China-Brazil Joint Laboratory for Space Weather (CBJLSW/NSSC/CAS). J Moro also thanks to CNPq/MCTI (Grant 429517/2018-01). J. Sousasantos greatly acknowledges FAPESP for support his research under grant (2018/06158-9) and NSF award AGS-1916055. C. S. Carmo and J. F. Campelo thanks to CNPq/MCTIC (Grants 141935/2020-3 and 123663/2021-0). S. S. Chen and G. A. Picanço thanks to CAPES/MEC (Grants 88887.362982/2019-00 and 88887.351778/2019-00).

We also thank the GSFC/SPDF OMNIWeb (https://omniweb.gsfc.nasa.gov) and the World Data Center for Geomagnetism, Kyoto (http://wdc.kugi.kyoto-u.ac.jp/) for make the data available. Data from the Brazilian Ionosonde network (São Luís, Fortaleza and Cachoeira Paulista) is made available through the EMBRACE program from the National Institute for Space Research (INPE) (http://www2.inpe.br/climaespacial/portal/ionosondes-home/). Data from digisonde installed in Port Stanley is available by Global Ionosphere Radio Observatory (GIRO) at DIDBase GIRO web Portal (https://ulcar.uml.edu/DIDBase/).

Appendix A. Supplementary material

Supplementary data to this article can be found online at https://doi.org/10.1016/j.asr.2023.02.020.

References

Abdu, M.A., Brum, C.G.M., Batista, I.S., Sobral, J.H.A., De Paula, E.R., Souza, J.R., 2008. Solar flux effects on equatorial ionization anomaly and total electron content over Brazil: observational results versus IRI representations. Adv. Space Res. 42 (4), 617–625. https://doi.org/10.1016/j.asr.2007.09.043.

Balogh, A., Southwood, D.J., Forsyth, R.J., Horbury, T.S., Smith, E.J., Tsurutani, B.T., 1995. The heliospheric magnetic field over the south polar region of the Sun. Science 268 (5213), 1007–1010. https://doi.org/10.1126/science.268.5213.1007.

Blanch, E., Altadill, D., 2012. Midlatitude F region peak height changes in response to interplanetary magnetic field conditions and modeling results. J. Geophys. Res.: Space Phys. 117 (A12). https://doi.org/10.1029/2012JA018009.

De Siqueira, P. M., De Paula, E. R., Muella, M. T. A. H., Rezende, L. F. C., Abdu, M. A., & Gonzalez, W. D. (2011, October). Storm-time total electron content and its response to penetration electric fields over South America. In Annales Geophysicae (Vol. 29, No. 10, pp. 1765-1778). Copernicus GmbH. Doi: 10.5194/angeo-29-1765-2011.

De Siqueira Negreti, P. M., de Paula, E. R., & Candido, C. M. N. (2017, December). Total electron content responses to HILDCAAs and geomagnetic storms over South America. In Annales Geophysicae (Vol. 35, No. 6, pp. 1309-1326). Copernicus GmbH. Doi: 10.5194/angeo-35-1309-2017, 2017.

Fedrizzi, M., Fuller-Rowell, T.J., Maruyama, N., Codrescu, M., Khalsa, H., 2008. Sources of F-region height changes during geomagnetic storms at mid latitudes. In: Kintner, P.M. (Ed.), Midlatitude Ionospheric Dynamics and Disturbances, Geophys. Monogr. Ser, vol. 181. AGU, Washington, D. C., pp. 247–258. https://doi.org/10.1029/181GM22.

Gonzalez, W.D., Guarnieri, F.L., Clua-Gonzalez, A.L., Echer, E., Alves, M.V., 2006. Magnetospheric energetics during HILDCAAs. In:

Tsurutani, McPherron, R., Lu, G., Sobral, J.H.A., Gopalswamy, N. (Eds.), 2018, Recurrent Magnetic Storms: Corotating Solar Wind Streams, 167. American Geophysical Union, Washington, DC, pp. 175–182. https://doi.org/10.1029/167GM15.

Guarnieri, F. L. (2006). The nature of auroras during high-intensity long-duration continuous AE activity (HILDCAA) events: 1998 to 2001. Recurrent magnetic storms: Corotating solar wind streams, 167, 235-243

Hajra, R., Echer, E., Tsurutani, B.T., Gonzalez, W.D., 2013. Solar cycle dependence of high-intensity long-duration continuous AE activity (HILDCAA) events, relativistic electron predictors? J. Geophys. Res. Space Phys. 118 (9), 5626–5638. https://doi.org/10.1002/jgra.50530.

Hajra, R., Tsurutani, B.T., Echer, E., Gonzalez, W.D., 2014. Relativistic electron acceleration during high-intensity, long-duration, continuous AE activity (HILDCAA) events: solar cycle phase dependences. Geophys. Res. Lett. 41 (6), 1876–1881. https://doi.org/10.1002/2014GL059383.

Jonah, O.F., De Paula, E.R., Muella, M.T.A.H., Dutra, S.L.G., Kherani, E.A., Negreti, P.M.S., Otsuka, Y., 2015. TEC variation during high and low solar activities over South American sector. J. Atmos. Sol. Terr. Phys. 135, 22–35. https://doi.org/10.1016/j.jastp.2015.10.005.

Koga, D., Sobral, J.H.A., Gonzalez, Arruda, D.C.S., Abdu, M.A., de Castilho, ... Zamlutti, C.J., 2011. Electrodynamic coupling processes between the magnetosphere and the equatorial ionosphere during a 5-day HILDCAA event. Journal of atmospheric and solar-terrestrial physics 73 (1), 148–155.

Liu, L., Chen, Y., 2009. Statistical analysis of solar activity variations of total electron content derived at jet propulsion laboratory from GPS observations. J. Geophys. Res.: Space Phys. 114 (A10). https://doi.org/10.1029/2009JA014533.

Mendillo, M., 2006. Storms in the ionosphere: patterns and processes for total electron content. Rev. Geophys. 44 (4). https://doi.org/10.1029/2005RG000193.

Prölss, G.W., Očko, M., 2000. Propagation of upper atmospheric storm effects towards lower latitudes. Adv. Space Res. 26, 131–135. https://doi.org/10.1016/S0273-1177(99)01039-X.

Reinisch, B.W., 1986. New techniques in ground-based ionospheric sounding and studies. Radio Sci. 21 (3), 331–341. https://doi.org/10.1029/RS021i003p00331.

Reinisch, B.W., Galkin, I.A., Khmyrov, G., Kozlov, A., Kitrosser, D., 2005. Automated collection and dissemination of ionospheric data from the digisonde network. Adv. Radio Sci. 2 (G. 1), 241–247. https://doi.org/10.5194/ars-2-241-2004.

Reinisch, B.W., Galkin, I.A., Khmyrov, G.M., Kozlov, A.V., Bibl, K., Lisysyan, I.A., Grochmal, J., 2009. New Digisonde for research and monitoring applications. Radio Sci. 44 (1). https://doi.org/10.1029/2008RS004115.

Sandanger, M.I., Soraas, F., Aarsnes, K., Oksavik, K., Evans, D.S., Greer, M.S., 2005. Proton injections into the ring current associated with Bz variations during HILDCAA events. Geophys. Monogr. – Am. Geophys. Union 155, 249. https://doi.org/10.1029/XXXGMXX.

Silva, R. P., Sobral, J. H. A., Koga, D., & Souza, J. R. (2017, October). Evidence of prompt penetration electric fields during HILDCAA events. In *Annales Geophysicae* (Vol. 35, No. 5, pp. 1165-1176). Copernicus GmbH. Doi: 10.5194/angeo-35-1165-2017.

Silva, R. P., Denardini, C. M., Marques, M. S., Resende, L. C. A., Moro, J., Silva Picanço, G. A. D., ... & Santos, M. A. F. D. (2020, January). Ionospheric total electron content responses to HILDCAA intervals. In Annales Geophysicae (Vol. 38, No. 1, pp. 27-34). Copernicus GmbH. Doi: 10.5194/angeo-38-27-2020.

Sobral, J.H.A., Abdu, M.A., Gonzalez, W.D., Gonzalez, A.C., Tsurutani, B.T., Da Silva, R.R., Guarnieri, F., 2006. Equatorial ionospheric responses to high-intensity long-duration auroral electrojet activity (HILDCAA). J. Geophys. Res.: Space Phys. 111 (A7). https://doi.org/10.1029/2005JA011393.

Søraas, F., Aarsnes, K., Oksavik, K., Sandanger, M.I., Evans, D.S., Greer, M.S., 2004. Evidence for particle injection as the cause of Dst reduction during HILDCAA events. J. Atmos. Sol. Terr. Phys. 66 (2), 177–186. https://doi.org/10.1016/j.jastp.2003.05.001.

Tsurutani, B.T., Ho, C.M., Smith, E.J., Neugebauer, M., Goldstein, B.E., Mok, J.S., Feldman, W.C., 1994. The relationship between interplanetary discontinuities and Alfvén waves: ulysses observations. Geophys. Res. Lett. 21 (21), 2267–2270. https://doi.org/10.1029/94GL02194.

Tsurutani, B.T., Gonzalez, W.D., 1987. The cause of high-intensity long-duration continuous AE activity (HILDCAAs): Interplanetary Alfvén wave trains. Planetary and Space Science 35 (4), 405–412.

Tsurutani, B.T., Gonzalez, W.D., Gonzalez, A.L.C., Tang, F., Arballo, J. K., Okada, M., 1995. Interplanetary origin of geomagnetic activity in the declining phase of the solar cycle. J. Geophys. Res. 100 (21), 717. https://doi.org/10.1029/95JA01476.

Tsurutani, B.T., Gonzalez, W.D., Guarnieri, F., Kamide, Y., Zhou, X., Arballo, J.K., 2004. Are high-intensity long-duration continuous AE activity (HILDCAA) events substorm expansion events? J. Atmos. Sol. Terr. Phys. 66 (2), 167–176. https://doi.org/10.1016/j.jastp.2003.08.015.

Wei, Y., Hong, M., Wan, W., Du, A., Lei, J., Zhao, B., Wang, W., Ren, Z., Yue, X., 2008. Unusually long lasting multiple penetration of interplanetary electric field to equatorial ionosphere under oscillating IMF Bz. Geophys. Res. Lett. 35, L02102. https://doi.org/10.1029/2007GL032305.

Yeeram, T., 2019. The solar wind-magnetosphere coupling and daytime disturbance electric fields in equatorial ionosphere during consecutive recurrent geomagnetic storms. J. Atmos. Sol. Terr. Phys. 187, 40–52. https://doi.org/10.1016/j.jastp.2019.03.004.

Yeeram, T., & Paratrasri, A. (2018, December). Recurrent geomagnetic storms and equinoctial ionospheric F-region in the low magnetic latitude: a case study. In Journal of Physics: Conference Series (Vol. 1144, No. 1, p. 012024). IOP Publishing. Doi: 10.1088/1742-6596/1144/1/012024.